Supplementary Information

S.I Summary of *g*-values Previously Reported in Crystalline Si

EPR has been used to characterize several defects in bulk *c*-Si. The intrinsic defects include vacancies and self-interstitials, and their agglomerates. Table S.1 lists some of the most common defects in *c*-Si and their respective *g*-values with the magnetic field oriented along the [100] direction of the *c*-Si lattice.

TABLE S.1 Defect centers found in bulk Si and their respective g-values along the [100] direction.

Defect Center	[100] g´ Tensor	Reference
A Center	2.0031	3, 4
Si-*E* Center	2.0070	5
G6 (positive divacancy)	2.0018, 2.0032	6
G7 (negative divacancy)	2.0085, 2.0120	6
Si-dangling bond	2.0055	7-9
E´ Center	2.0005	10
P_b Center	2.002–2.008	10
Si-A14	2.0022	11
Si-A15	2.0045	11
Si-A16	2.0036	11
Si-P2	2.0020	12
Si-P4	2.0041	12
Si-P5	2.0050	12

S.II Confirmation of Observation of Boron Acceptors in Broad Magnetic Field EPR Scans

The EPR spectrum for unionized B acceptors was first observed by Feher *et al.* under high mechanical stress,[1] and is shown Figure S.1 along with our experimental data for B-doped Cz Si in the "degraded" state of LID. The large features in both spectra between ~200–600 mT confirm that the features observed in our broad magnetic field scans are due to frozen out boron acceptors. [13]

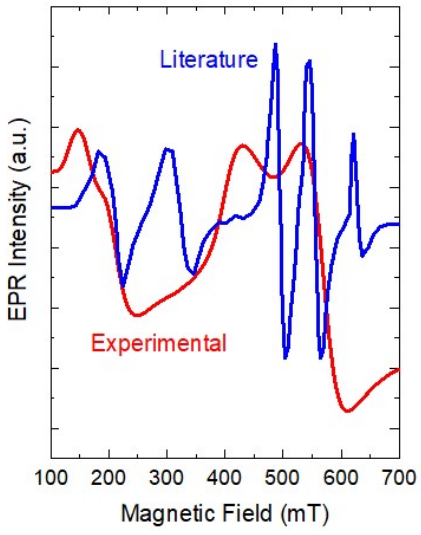

FIG S.1 Broad magnetic field EPR spectrum of boron acceptors from the literature (—) [1] and our experimental data (—).

S.III Observation of No Boron Acceptor Fine Structure in *n*-type Cz Si

0Figure S.2 shows broad range EPR spectra of phosphorous-doped Cz Si before and after light exposure. It can be seen that there is no broad EPR signatures due to boron acceptor before or after light exposure.

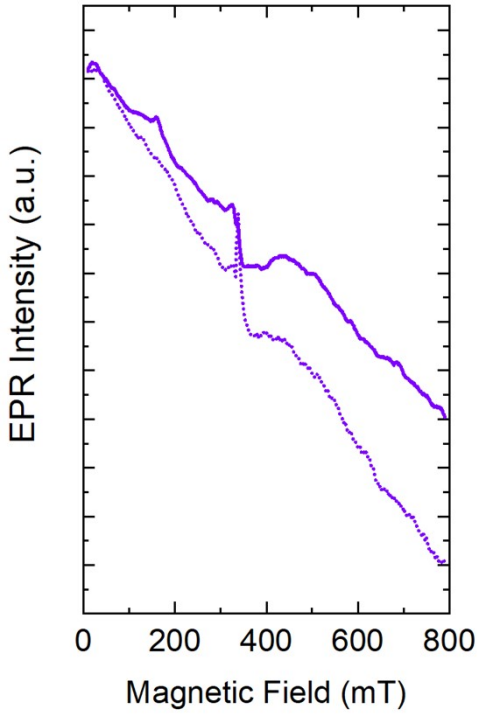

FIG. S.2. Broad range EPR spectra before (—) and after (---) light-exposure of phosphorous-doped Cz Si.

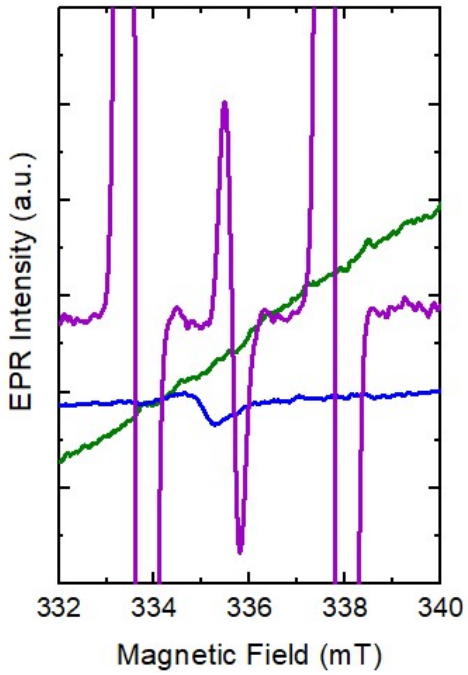

FIG. S.3. Narrow range EPR spectra after light-exposure of boron-doped Cz Si (—), boron-doped FZ Si (—), and phosphorus-doped Cz Si (—).

S.IV Effect of Material Doping and Oxygen Concentration on Narrow Magnetic EPR Scans after Light Exposure

To further confirm that the narrow-range EPR signature at ~335 mT is due to the BO LID defect, we also recorded EPR spectra of "degraded" B-doped FZ Si and P-doped Cz Si samples. Figure S.3 shows narrow magnetic field range scans of *p*-type Cz Si (—), *p*-type FZ Si (—), and *n*-type Cz Si (—) after 24 hr of illumination at 1 Sun at room temperature. The EPR spectrum for the *p*-type Cz Si sample shows an EPR feature at ~335 mT, which is related to the LID defect. In contrast, the EPR spectrum for the *p*-type FZ Si sample is relatively featureless and does not exhibit the same EPR signature at 335 mT. Finally, the *n*-type Cz Si sample has three distinct features before and after light-exposure. The two outer, high intensity, signatures are attributed to isolated phosphorous atoms and the middle peak, with a lesser intensity, is attributed to phosphorus pairs.[14] It is important to note that these EPR signatures in the *n*-type Cz Si samples are independent of light exposure.

S.V Effect of Orientation of B-doped Cz Si Samples in the Degraded State of LID for Narrow-Range Magnetic Field EPR Scans

Figure S.4 shows the narrow magnetic field EPR spectra of the B-doped Cz Si sample in the fully "degraded" state of LID in different loading orientations with respect to the magnetic field. In all EPR spectra, we observe an EPR signature related to LID located at ~334 mT. We show that the g-value of the EPR signature is independent of loading orientation, which we attribute to large amounts of random strain in the sample.

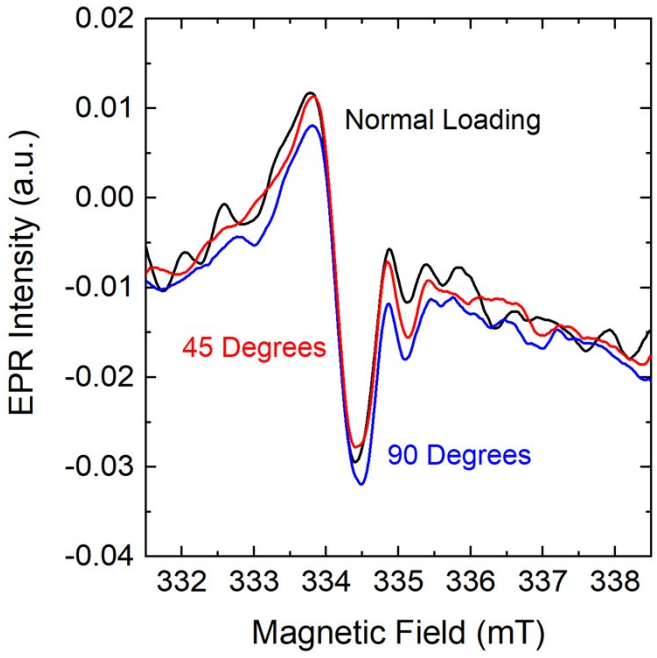

FIG S.4. Narrow range EPR spectra after light-exposure of *p*-Cz Si with the magnetic field oriented parallel (—), at 45° (—), and at 90° (—) with respect to the Si [100] direction in the EPR cavity.

References

[1]H. Neubrand, Phys. Status Solidi B-Basic Res. **86** (1), 269-275 (1978).
[2]S. Wilking, C. Beckh, S. Ebert, A. Herguth and G. Hahn, Sol. Energy Mater. Sol. Cells **131**, 2-8 (2014).
[3]G. D. Watkins, J. W. Corbett and R. M. Walker, J. Appl. Phys. **30** (8), 1198-1203 (1959).
[4]J. W. Corbett, G. D. Watkins, R. M. Chrenko and R. S. McDonald, Physical Review **121** (4), 1015-& (1961).
[5]G. D. Watkins and J. W. Corbett, Physical Review **134** (5A), 1359-+ (1964).
[6]G. D. Watkins and J. W. Corbett, Physical Review **138** (2A), A543-+ (1965).
[7]T. J. McMahon and Y. Xiao, Appl. Phys. Lett. **63** (12), 1657-1659 (1993).
[8]Y. Fu and P. A. Fedders, Solid State Commun. **84** (8), 799-801 (1992).
[9]M. Stutzmann and D. K. Biegelsen, Phys. Rev. B **40** (14), 9834-9840 (1989).
[10]P. M. Lenahan and J. F. Conley, J. Vac. Sci. Technol. B **16** (4), 2134-2153 (1998).
[11]Y. H. Lee and J. W. Corbett, Phys. Rev. B **13** (6), 2653-2666 (1976).
[12]W. Jung and G. S. Newell, Physical Review **132** (2), 648-& (1963).
[13]H. Neubrand, Phys. Status Solidi B-Basic Res. **90** (1), 301-308 (1978).
[14]A. M. Tyryshkin, S. A. Lyon, A. V. Astashkin and A. M. Raitsimring, Phys. Rev. B **68** (19), 4 (2003).